ELSEVIER

Ceramics International 30 (2004) 1435–1442

CERAMICS INTERNATIONAL

www.elsevier.com/locate/ceramint

Effects of chemical modification on the electrical properties of $0.67BiFeO_3-0.33PbTiO_3$ ferroelectric ceramics

W.M. Zhu, Z.-G. Ye*

Department of Chemistry, Simon Fraser University, 8888 University Drive, Burnaby, BC, Canada V5A 1S6

Received 3 December 2003; received in revised form 18 December 2003; accepted 23 December 2003

Available online 10 May 2004

Abstract

Ceramics of the $BiFeO_3-PbTiO_3$ solid solution are expected to exhibit interesting ferroelectric and magnetoelectric properties. In this work, chemical modifications are carried out in order to improve the dielectric performance of the materials. Ceramics of $0.67BiFeO_3-0.33PbTiO_3$, $0.67BiFe_{0.98}Ti_{0.02}O_3-0.33PbTiO_3$ (via B site Ti^{4+} modification) and $0.67BiFeO_3-0.33PbTiO_3$ sintered under O_2 flow are synthesised. The frequency-dependence of the impedance is measured at various temperatures and analysed. It is found that the dielectric properties are improved by B site Ti^{4+} modification and by sintering in O_2 flow. The temperature dependences of dc conductivity of the grains for the three ceramic samples are derived from impedance analysis by fitting their impedance data to an electric equivalent circuit of three RC components. The temperature dependences of both the dc conductivity of the grains and the measured ac conductivity (at high and low frequencies) show that the conductivity for O_2-sintered sample is the lowest, and the conductivity of $0.67BiFe_{0.98}Ti_{0.02}O_3-0.33PbTiO_3$ is lower than that of $0.67BiFeO_3-0.33PbTiO_3$. This result is consistent with the dielectric properties of the respective ceramics. The mechanism of the electric conduction is discussed in relation to the chemical modifications and related defect chemistry.

Keywords: B. Spectroscopy; B. X-ray method; C. Electrical conductivity; C. Dielectric properties

1. Introduction

The $(1-x)BiFeO_3$–$xPbTiO_3$ solid solution of perovskite structure with compositions near the morphotropic phase boundary (MPB) ($x = 0.3$–0.35) shows a huge tetragonality (lattice parameter ratio c/a) in its tetragonal phase [1–3], which theoretically predicts large electric polarisation [3]. The ferroelectric Curie point of the MPB compositions derived from high temperature X-ray diffraction is around 700 °C [4], indicating the potential of this system for high temperature applications using piezo- and ferroelectric properties. Experimentally, due to high electric conductivity [3,4], the dielectric constant of this system can only be measured at high frequencies and at temperatures lower than 500 °C [4], or with the aid of a special technique of ultrahigh frequency measurement [2], and no data on the electric polarisation were reported. On the other hand, little work has focused on the electric conduction study for this system. The only conductivity measurement on ceramic sample [4] showed that the dc conductivity of the MPB composition is only one order of magnitude higher than that of $PbTiO_3$ ceramic, which is lower than expected from the dielectric results of the $(1-x)BiFeO_3$–$xPbTiO_3$ ceramics. So it is interesting to study the electric conduction behaviour in this system, which will be helpful for improving the dielectric properties by decreasing the electric conductivity of this system. Aliovalent doping and annealing (or sintering) in a certain atmospheric environment are commonly used to modify the conductivity by changing the concentration of conduction species [5]. Being an ionic compound, the $BiFeO_3$–$PbTiO_3$ solid solutions may have high energy gap between valence band and conduction band, so that electrons could not be thermally activated easily in the temperature interval of measurement ($\leq$550 °C in our case). Therefore, the conductivity in this system is expected to result mainly from the presence of defects, which introduce extrinsic (donor and/or acceptor) levels allowing electrons to be thermally activated. In this work, we use chemical modifications to change the concentration of some defects in the ceramics. The dielectric properties and electric con-

* Corresponding author. Fax: +1-604-291-3765.
E-mail address: zye@sfu.ca (Z.-G. Ye).

0272-8842/$30.00
doi:10.1016/j.ceramint.2003.12.072

ductivities of the modified ceramics are characterised and compared with those of the unmodified ceramics.

For ceramic samples, the study of electric conduction behaviour based on direct dc conductivity measurement may be complicated because of the fact that the measured dc conductivity usually comes from different electric components, namely, grain, grain boundary and interface between the sample and electrodes. As a result, the measured dc conduction is usually an overall result. The conduction behaviour of the grains can be quite different from that of the grain boundary. Furthermore, when measuring dc electric conductivity, high electric field is usually applied on the sample in order to meet the instrumental resolution for the current measurement when the resistivity of the sample is relatively high at low temperature, which, for ferroelectric material, will induce large electric polarisation change, making the situation more complicated. Impedance spectroscopy measures the current response of a sample when applying a small ac signal, in which the electric field of the ac signal is low enough so that no significant polarisation change is induced in ferroelectric material. Impedance analysis in frequency domain is a powerful tool to separate the different components in a ceramic by identifying the different RC elements and assigning them to appropriate regions of the sample [6,7]. In this work, we apply the impedance spectroscopy to deduce the resistance of the grains, and to study the conduction mechanism of $BiFeO_3$–$PbTiO_3$ ceramics.

2. Experimental

Three ceramic samples: (i) $0.67BiFeO_3$–$0.33PbTiO_3$ (nominally pure, denoted as BF–PT), (ii) $0.67BiFe_{0.98}Ti_{0.02}O_3$–$0.33PbTiO_3$ (B site Ti^{4+} substitution for Fe^{3+}, denoted as BFT–PT) and (iii) $0.67BiFeO_3$–$0.33PbTiO_3$ sintered in oxygen flow (denoted as BF–PT(O)), were prepared by conventional solid state reactions. Bi_2O_3 (99.975%), PbO (99.99%), Fe_2O_3 (99%) and TiO_2 (99.9%) were weighted according to the chemical formula of each composition, mixed and ground in a mortar for 3 h. The powders were then pressed into discs and calcined at 800 °C for 2 h. After calcination, samples were ground for 3 h with a few drops of 5% polyvinyl alcohol as binder, pressed into pellets, then heated at 700 °C for 1 h to eliminate the binder. For the BF–PT and BFT–PT samples, the pellets were then sintered in a sealed Al_2O_3 crucible at 1040 °C for 1 h. For the BF–BT(O) sample, the pellet was put on a Pt plate and placed into a horizontal tube furnace to be sintered in oxygen flow. Both ends of the tube furnace were covered with alumna lids having a tube in the centre. The inlet tube was connected to an oxygen tank. The oxygen flow from the outlet tube was equilibrated with atmosphere, so that the oxygen partial pressure inside the furnace was 1 atm. After sintering, the surfaces of the samples were polished and the thickness reduced to about 1 mm. The phases were checked by XRD using a Philips PW 1730 diffractometer with a Cu Kα source. The lattice parameters were refined from the XRD profiles using "xlat" program. The pellets were then sputtered with gold layers as electrodes for characterisation. The impedance spectra were measured by a Solartron 1260 impedance analyser combined with a Solartron 1296 dielectric interface, in a frequency range of 10–10^6 Hz with a voltage of 0.5 V (peak to peak). The dielectric constant, dissipation factor ($\tan\delta$) and ac conductivity were extracted from the impedance data. The measured impedance data were fitted to an equivalent electric circuit using "Zview2" program.

3. Results and discussion

3.1. Synthesis

Fig. 1 shows the XRD spectra of the BF–PT, BFT–PT and BF–PT(O) ceramics. It can be seen that, at room temperature, all three samples have a perovskite structure with the coexistence of the tetragonal and rhombohedral phases, which is the characteristic of the MPB behaviour. The rhombohedral phase component increases by the modifications, as evidenced by the increase of the intensity of R(1 0 –1) peak of both BFT–PT and BF–PT(O) compared with that of BF–PT. The lattice parameters of the tetragonal phase for the three samples are listed in Table 1. The c/a ratio of the tetragonal phase is found to be 1.1674(7) for BF–PT, 1.1272(10) for BFT–PT and 1.1598(8) for BF–PT(O), respectively. The c/a ratio confirms the large lattice distortion in this system. The tetragonality (c/a) decreases significantly in BFT–PT as a result of the substitution of Ti^{4+} for Fe^{3+} on the B site, resulting from the difference in ionic radii ($r(Ti^{4+}) = 0.605$ Å, $r(Fe^{3+}) = 0.645$ Å).

3.2. Dielectric properties

The dielectric properties of the $BiFeO_3$–$PbTiO_3$ ceramics appear very complicated because of electric conduction. As shown in Fig. 2, several anomalies were found on the temperature dependence of the dielectric constant (ε') for all the three samples, namely, one at around 170 °C for BF–PT(O), 210 °C for BF–PT, 270 °C for BFT–PT, and another one at 420 °C for BF–PT and BF–PT(O). At the same time, the dielectric constant drops to negative value at $T > 350$ °C at all frequencies for BF–PT while only at low frequency (10^2 Hz) for BFT–PT and BF–PT(O), and the temperature

Table 1
Lattice parameters of tetragonal phase for the BF–PT, BFT–PT and BF–PT(O) ceramics at room temperature

	a (Å)	c (Å)	c/a
BF–PT	3.8320(10)	4.4733(26)	1.1674(7)
BFT–PT	3.8445(20)	4.3336(33)	1.1272(10)
BF–PT(O)	3.8334(18)	4.4461(25)	1.1598(8)

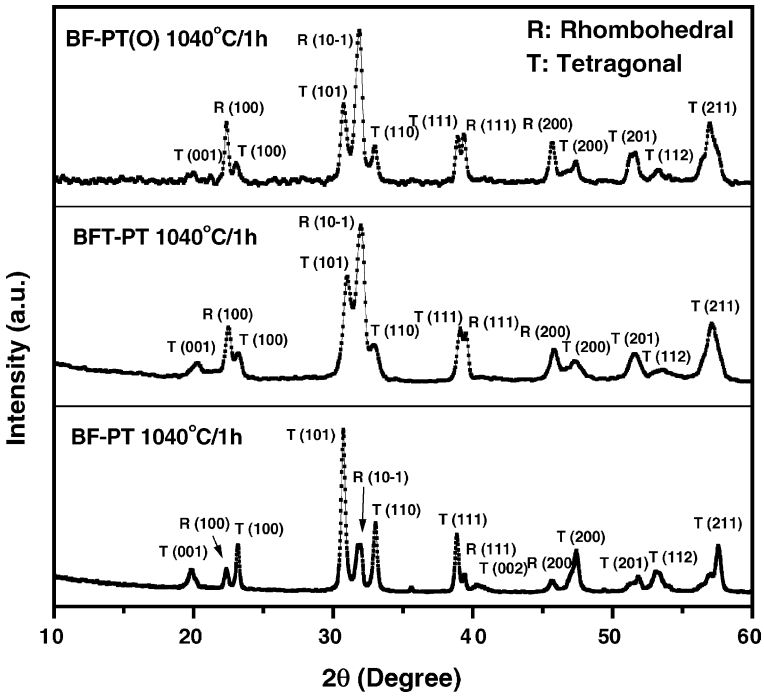

Fig. 1. XRD patterns for the BF–PT, BFT–PT and BF–PT(O) ceramics sintered at 1040 °C for 1 h.

at which the drop starts is higher for BF–PT(O) than for BFT–PT.

These anomalies of dielectric constant seem to agree with the dielectric measurements by Krainik et al. [8], who found eight anomalies in $BiFeO_3$ ceramic from room temperature to ferroelectric Curie point, but the nature of these anomalies was not explained. No information can be found in literature to explain the anomalies at around 170, 210 and 430 °C measured in our samples. The anomaly at around 270 °C corresponds to the anti-ferromagnetic to paramagnetic phase transition at Neel temperature (T_N), according to the phase diagram of this system [1]. This phase transition is more clearly observed on $\tan\delta$ versus temperature relations (Fig. 3), where all three samples show the anomaly at around 270 °C at different frequencies. This dielectric anomaly appearing at a magnetic phase transition implies a magneto-electric coupling in this system.

The drop of dielectric constant to negative value is due to high electric conduction in the sample, which makes the phase angle of ac current response too small to be measured by the instrument, giving rise to an error data (negative ε'). It

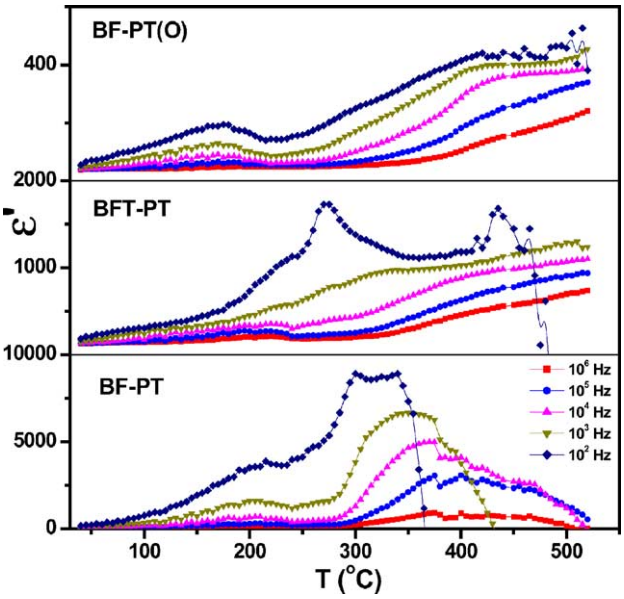

Fig. 2. Temperature dependence of the dielectric constant at various frequencies for the BF–PT, BFT–PT and BF–PT(O) ceramics.

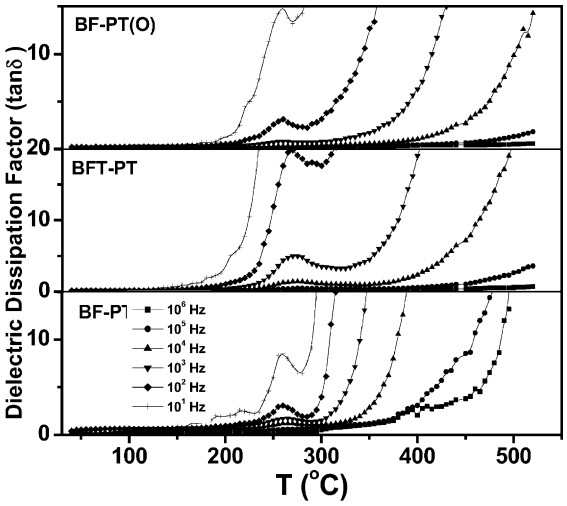

Fig. 3. Temperature dependence of the dielectric dissipation factor ($\tan\delta$) at various frequencies for the BF–PT, BFT–PT and BF–PT(O) ceramics.

Table 2
Dielectric constant (ε') and dissipation factor ($\tan\delta$) at room temperature for the BF–PT, BFT–PT and BF–PT(O) ceramics at different frequencies

		10^2 Hz	10^3 Hz	10^4 Hz	10^5 Hz	10^6 Hz
BF–PT	ε'	166	117	105	101	99
	$\tan\delta$	0.427	0.185	0.0557	0.0251	0.0398
BFT–PT	ε'	185	146	134	130	126
	$\tan\delta$	0.186	0.113	0.0375	0.0252	0.0349
BF–PT(O)	ε'	55	46	41	40	38
	$\tan\delta$	0.239	0.136	0.04	0.0155	0.0833

can be seen that the meaningful (positive) dielectric constant can be measured up to much higher temperature in BFT–PT and BF–PT(O) than in BF–PT. Table 2 shows the room temperature ε' and $\tan\delta$ values of the three samples measured at different frequencies. The $\tan\delta$ values of BFT–PT and BF–PT(O) are lower than that of BF–PT at all frequencies except for 10^6 Hz. The ε' value of BF–PT(O) is lower than that of BF–PT. The decease ε' in BF–PT(O), together with the decrease of $\tan\delta$, suggests that the measured ε' of unmodified BF–PT must contain an appreciable contribution from electric conduction. BFT–PT, however, shows a higher ε' and a lower $\tan\delta$ than BF–PT, which implies that the substitution of the ferroelectric active Ti^{4+} for Fe^{3+} on the B site enhances the dielectric properties of this system. The decreases of $\tan\delta$ and ε' by chemical modifications is even more significant as temperature increases, as shown in Figs. 4 and 5, respectively. At high temperatures ($T > 225\,^\circ$C), the ε' of BF–PT becomes larger than that of BFT–PT (Fig. 5), resulting from an overwhelming contribution of electric conduction. All these results indicate that the dielectric properties of BF–PT are improved by chemical modifications via a significant reduction of the electric conduction.

The ac conductivity derived from the impedance data of the three samples shows a sequence of σ_{ac} (BF–PT(O)) < σ_{ac} (BFT–PT) < σ_{ac} (BF–PT) for low (10^2 Hz) and high (10^5 Hz) frequencies in the temperature range of measurement, except for near T_N (Fig. 6). This means that the overall ac electric conductivity is decreased in the modified $0.67BiFeO_3$–$0.33PbTiO_3$ ceramics. Detailed information on conductivity (i.e. conductivity of the grain, grain boundary, etc.), dc conductivity and conduction mechanism will be discussed in the next section.

3.3. Impedance spectroscopy

The impedance of some ferroelectric materials can be fitted by an equivalent circuit composed of a series array of parallel RC elements [6], as illustrated in Fig. 7. In practice, to determine the number of RC elements in the circuit, a physical model for the material is usually suggested with each component in the material representing an RC element in the circuit. This circuit needs to fit the experimental impedance data, otherwise, the physical model should be revised, and the number of RC element should be changed

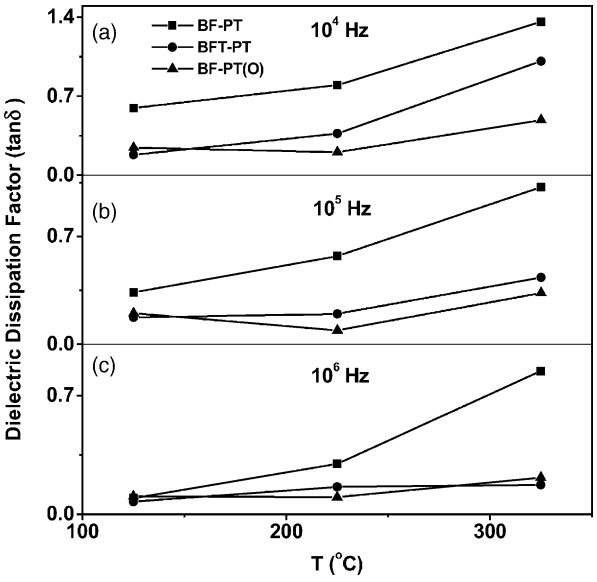

Fig. 4. Comparison of the dielectric dissipation factor ($\tan\delta$) among the BF–PT, BFT–PT and BF–PT(O) ceramics at different temperatures and frequencies.

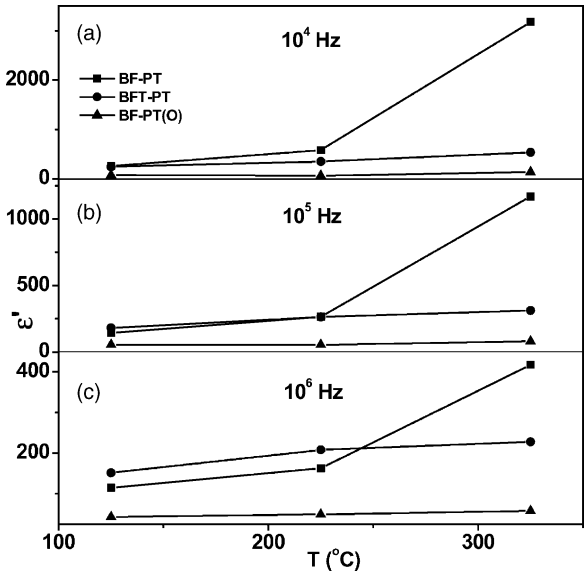

Fig. 5. Comparison of the dielectric constant (ε') among the BF–PT, BFT–PT and BF–PT(O) ceramics at different temperatures and frequencies.

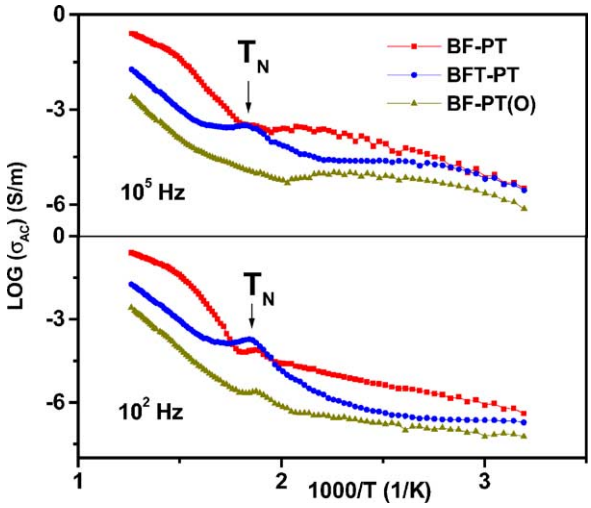

Fig. 6. Temperature dependence of ac conductivity for the BF–PT, BFT–PT and BF–PT(O) ceramics.

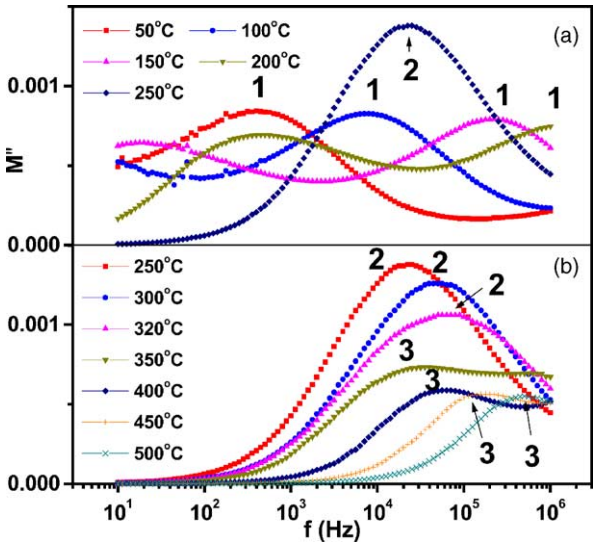

Fig. 8. Frequency dependences of the imaginary part of the electric modules (M'') at different temperatures for the BFT–PT ceramic.

until the experimental data fits. Sometimes, the information for setting up the circuit can also be derived by the inspection of impedance and/or electric modulus data in frequency domain. Since each RC element has a characteristic relaxation time determined by the relation, RC $= \tau$, it should show a peak at its relaxation frequency on the imaginary part of impedance (Z'') and electric modulus (M'') spectra in frequency domain if the difference of the product of R and C among these RC elements is large enough [6].

Fig. 8 shows the M'' dependence on frequency for BFT–PT as an example. In the low temperature region (Fig. 8a), peak 1 moves to high frequency as temperature increases, with its amplitude unchanged. This means that the capacitance of the corresponding RC element is temperature independent, while the resistance decreases with the increase of temperature, which is the characteristic of grain boundary behaviour. As peak 1 moves to higher frequencies, a second peak (peak 2) becomes observable at low frequencies as temperature increases to 150 and 200 °C. At 250 °C, however, this peak shows a much larger amplitude at $f = 2 \times 10^4$ Hz. In the high temperature region above 250 °C (Fig. 8b), peak 2 becomes broadened and then tends to split into two peaks, so that a third peak (peak 3) appears at $T \geq 350$ °C. At the same time, both peak 2 and peak 3 shift to higher frequencies and the amplitude of the peaks decreases as temperature increases. Therefore, at $T \geq 350$ °C, two RC elements could be deduced from Fig. 8b (peak 3 and the other peak at higher frequency from the split of peak 2). Together with peak 1 (that has travelled to much higher frequencies and thus is no longer observable in the frequency range in Fig. 8b), the equivalent circuit of the materials at high temperature can be composed of three RC elements. For the RC element corresponding to peak 3, the capacitance increases and the resistance decreases with the increase of temperature.

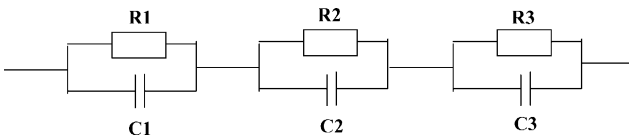

Fig. 7. Proposed equivalent circuit for the BF–PT, BFT–PT and BF–PT(O) ceramics.

Fitting of the impedance data of the three samples was then performed based on the equivalent circuit with three RC elements (Fig. 7). Fig. 9 gives selected impedance data and fitting results for temperature higher than 350 °C, showing that fitting is satisfactory for all three samples. However, at temperatures lower than 350 °C, some deviations arise (not shown). This is probably because at temperatures higher than 350 °C, the two peaks split from peak 2 are separated enough so that they are well defined, while at temperatures lower than 350 °C, the two peaks are almost merged together and indistinguishable (Fig. 8b). The capacitances and resistances for each element of the three samples are derived from fitting. The capacitances of the three samples as a function of temperature are plot in Fig. 10, which clearly shows that C3 for all the three samples increases with temperature, and C1 and C2 are basically temperature independent except in BF–PT(O), where C1 and C2 increase slightly with increasing temperature. Therefore, we assign C3 as the capacitance of the grains of the ferroelectric material whose capacitance increases with temperature below the Curie point, and accordingly, R3 is assigned the resistance of the grains. Fig. 11 shows the Arrhenius plots of R3 for the three samples, the slopes of which indicate the activation energies E_a. It is found that E_a values for the grains of the three samples are very close: $E_a = 1.39$ eV for BF–PT, 1.39 eV for BFT–PT and 1.30 eV for BF–PT(O), respectively. At a given temperature, the dc electric conductivity σ_{dc} has a sequence of σ_{dc} (BF–PT(O)) $< \sigma_{dc}$ (BFT–PT) $< \sigma_{dc}$ (BF–PT). These results

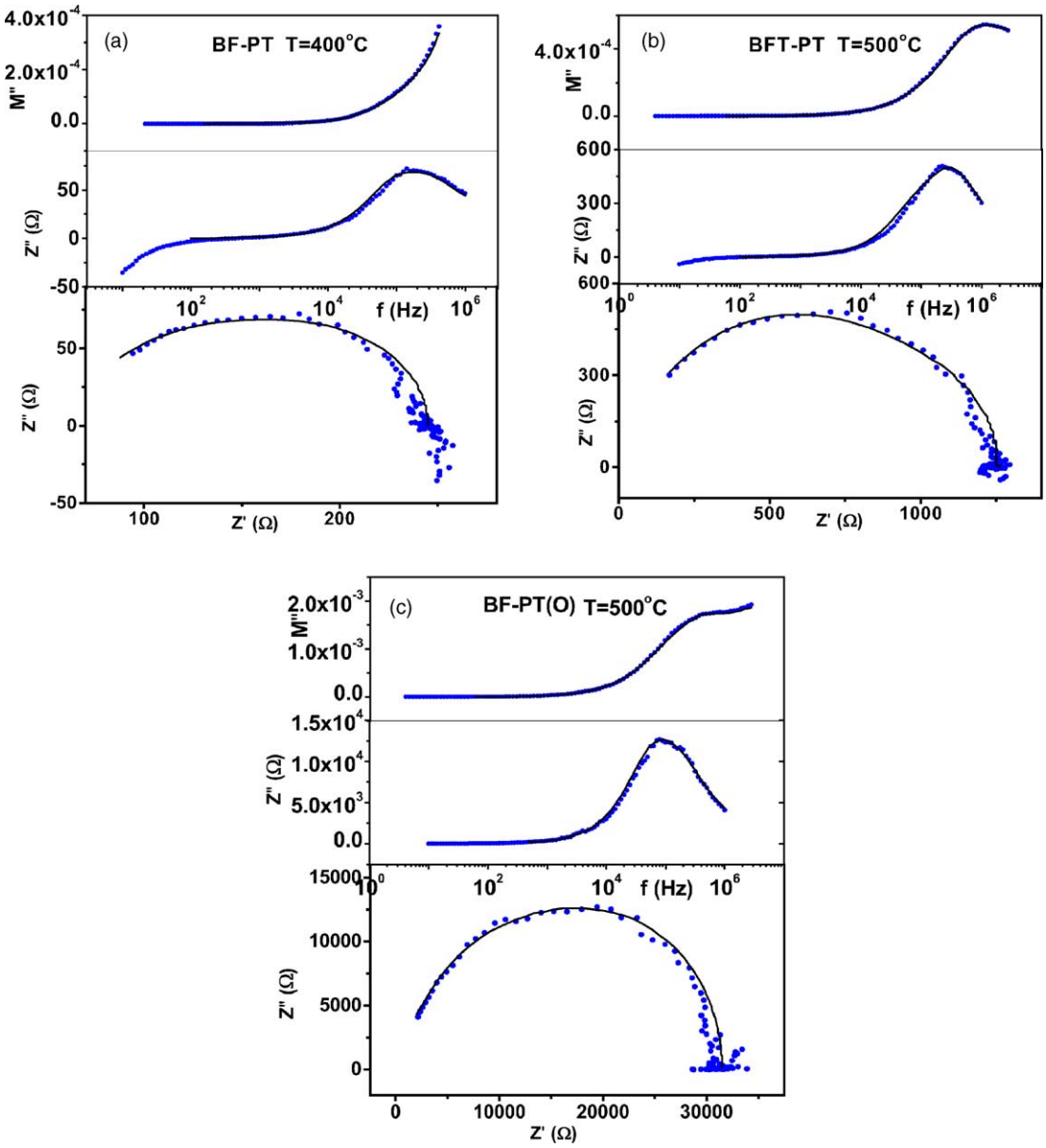

Fig. 9. Impedance data (points) and fitting (solid lines) to the equivalent circuit of three RC elements (shown in Fig. 7) for the BF–PT (a), BFT–PT (b) and BF–PT(O) (c) ceramics.

indicate that the three samples are of the same conduction mechanism, but the conductivity of BFT–PT is lower than that of BF–PT, and the conductivity of BF–PT(O) is the lowest.

3.4. Conduction mechanism

Electric conduction is in general composed of electronic conduction and ionic conduction. For the $BiFeO_3$–$PbTiO_3$ ceramics, the electronic conduction in the grains is expected to result mainly from the defects presented in the lattice. These defects could come from the volatilisation of PbO and/or Bi_2O_3 during materials preparation process, which could result in oxygen vacancies, lead and bismuth vacancies and the defect associates, i.e. (V_{Pb}–V_O) and (V_{Bi}–V_O). In addition, the presence of lower-charged impurities for transition elements, especially Fe^{2+}, is unavoidable for their natural abundance [9,10]. As a result, both Fe^{2+} and oxygen vacancies are present to satisfy the electric neutrality according to the reaction using Kröger–Vink notation:

$$\begin{aligned} &Bi_2O_3 + (1-\delta)Fe_2O_3 + 2\delta FeO + PbO + TiO_2 \\ &\quad \rightarrow 2BiFe^{3+}_{1-\delta}Fe^{2+}_{\delta}O_{3-\delta/2}V_{O\delta/2} + PbTiO_3 \\ &\qquad [2Bi^{x}_{Bi} + (2-2\delta)Fe^{x}_{Fe} + 2\delta Fe'_{Fe} + Pb^{x}_{Pb} + Ti^{x}_{Ti} \\ &\qquad + (9-\delta)O^{x}_{O} + \delta V^{2+}_{O}] \end{aligned}$$

where Bi^{x}_{Bi} stands for a Bi^{3+} ion occupying Bi^{3+} site, Fe^{x}_{Fe} for a Fe^{3+} ion occupying Fe^{3+} site, Fe'_{Fe} for a Fe^{2+} ion oc-

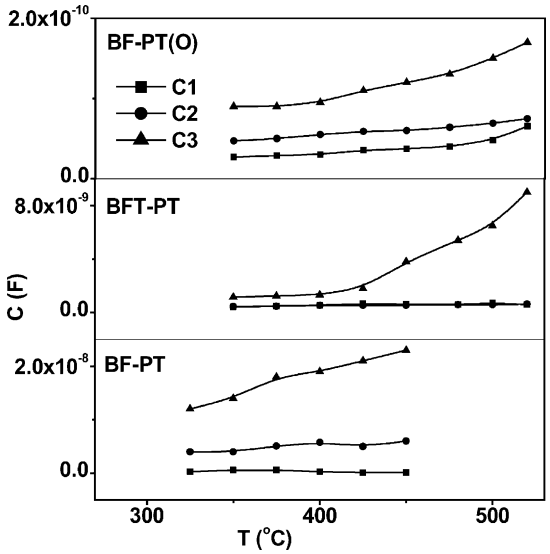

Fig. 10. Temperature dependence of the fitted capacitance for the BF–PT, BFT–PT and BF–PT(O) ceramics.

cupying Fe^{3+} site with a negative charge, Pb^{x}_{Pb} for a Pb^{2+} ion occupying Pb^{2+} site, Ti^{x}_{Ti} for a Ti^{4+} ion occupying Ti^{4+} site, O^{x}_{O} for a O^{2-} ion occupying O^{2-} site, V^{2+}_{O} for an oxygen vacancy with positive charge. The presence of Fe^{2+} may lead to electron hopping conduction from Fe^{2+} to Fe^{3+}, as known in materials with spinel structure, e.g. Fe_3O_4, in which Fe^{2+} occupies octahedral site, Fe^{3+} occupies both octahedral and tetrahedral sites [11]. The octahedrons and tetrahedron share faces, so it is easy for electrons to hop from Fe^{2+} to Fe^{3+}. In $BiFeO_3$–$PbTiO_3$ of perovskite structure, however, both Fe^{2+} and Fe^{3+} occupy the octahedral site, and the octahedrons in perovskite are connected by vertices, so that there is one O^{2-} in between Fe^{2+} and Fe^{3+}, which blocks the direct hopping of electrons from Fe^{2+} to Fe^{3+}. Nevertheless, the hopping of electrons becomes possible in these materials when oxygen vacancies are present, which act as "bridge" between Fe^{2+} and Fe^{3+}. The oxygen vacancies carrying positive charge attract electrons from Fe^{2+}, but

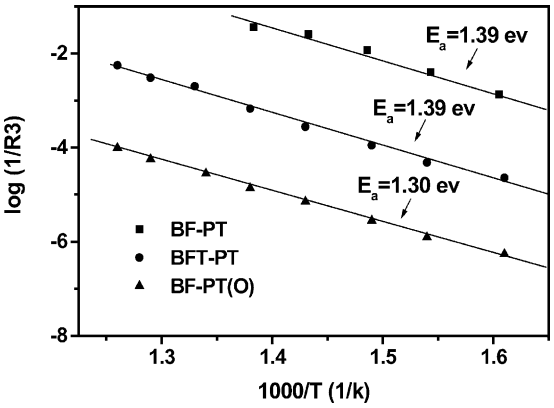

Fig. 11. Arrhenius plots of R3 for the BF–PT, BFT–PT and BF–PT(O) ceramics.

they are not effective electron traps even at room temperature [9], so electrons can easily escape from the oxygen vacancies traps and hop to Fe^{3+}. Based on this consideration, it is reasonable to believe that the hopping of electrons from Fe^{2+} to Fe^{3+} plays an important role in the electronic conduction for the $BiFeO_3$–$PbTiO_3$-based ceramics. BF–PT(O) exhibits the lowest conductivity since the concentration of both Fe^{2+}, the source of charge carriers, and oxygen vacancies, the bridging species, are decreased by sintering in oxygen flow:

$$2\ BiFe^{3+}_{1-\delta}Fe^{2+}_{\delta}O_{3-\delta/2}V_{O\delta/2} + PbTiO_3[2Bi^{x}_{Bi} + (2-2\delta)Fe^{x}_{Fe} + 2\delta Fe'_{Fe} + Pb^{x}_{Pb} + Ti^{x}_{Ti} + (9-\delta)O^{x}_{O} + \delta V^{2+}_{O}] + \frac{\delta}{2}O_2 \rightarrow 2BiFeO_3 + PbTiO_3[2Bi^{x}_{Bi} + 2Fe^{x}_{Fe} + Pb^{x}_{Pb} + Ti^{x}_{Ti} + 9O^{x}_{O}]$$

For BFT–PT, the concentration of oxygen vacancies are reduced by the substitution of Ti^{4+} for Fe^{3+} on the B site:

$$2BiFe^{3+}_{1-\delta}Fe^{2+}_{\delta}O_{3-\delta/2}V_{O\delta/2} + PbTiO_3[2Bi^{x}_{Bi} + (2-2\delta)Fe^{x}_{Fe} + 2\delta Fe'_{Fe} + Pb^{x}_{Pb} + Ti^{x}_{Ti} + (9-\delta)O^{x}_{O} + \delta V^{2+}_{O}] + 2\delta TiO_2 \rightarrow 2BiFe^{3+}_{1-2\delta}Fe^{2+}_{\delta}Ti^{4+}_{\delta}O_3 + PbTiO_3 [2Bi^{x}_{Bi} + (2-4\delta)Fe^{x}_{Fe} + 2\delta Fe'_{Fe} + 2\delta Ti^{+}_{Fe} + Pb^{x}_{Pb} + Ti^{x}_{Ti} + 9O^{x}_{O}] + \delta Fe_2O_3$$

As a result, the conductivity for BFT–PT is lower than that of BF–PT, in agreement with the Arrhenius plots for the grains of the three samples. This indicates that the Ti^{4+} substitution rate chosen was adequate in reducing the conductivity of $0.67BiFeO_3$–$0.33PbTiO_3$ ceramic, since an over doping would increase the amount of Fe^{2+}, thus increasing the conductivity.

In perovskite oxides, the only possible ionic conduction comes from the migration of oxygen vacancies [9,12], which, if present, would lead to a spike on the complex impedance plots at low frequency. The diffusion of oxygen vacancies into the electrodes would give rise to a large resistance at the ceramic electrode interface, which appears as a spike on the complex impedance plots [6]. However, no such spike is found for any of the three samples (Fig. 8). Therefore, the ionic contribution from the migration of oxygen vacancies to the electric conduction of $BiFeO_3$–$PbTiO_3$ ceramics is not significant.

4. Conclusions

Chemical modifications have been performed on the $0.67BiFeO_3$–$0.33PbTiO_3$ ceramics by B site Ti^{4+} substitution for Fe^{3+} and by sintering the ceramics in oxygen flow. The dc electric conductivity for the grains of the $0.67BiFeO_3$–$0.33PbTiO_3$, Ti^{4+}-modified $0.67BiFe_{0.98}Ti_{0.02}O_3$–$0.33PbTiO_3$ and O_2-sintered $0.67BiFeO_3$–$0.33PbTiO_3$ ceramics were extracted by the impedance spectra analysis.

Both the dc electric conductivity for the grains and the overall ac electric conductivity of $0.67BiFeO_3$–$0.33PbTiO_3$ ceramic are found to decrease either by Ti^{4+}-substitution for Fe^{3+} on the B site or by sintering in oxygen flow. The chemical modifications do not change the electric conduction mechanism in these ceramics systems, which mainly originates from the hopping of electrons from Fe^{2+} to Fe^{3+} without significant contribution from ionic conduction. The chemical modifications performed in this work are proved to be effective in improving the dielectric properties of $BiFeO_3$–$PbTiO_3$ solid solution materials for potential high temperature piezoelectric and magneto-electric applications.

Acknowledgements

This work was supported by the US Office of Naval Research (Grant No. N00014-99-1-0378).

References

[1] S.A. Fedulov, P.B. Ladyzhinskii, I.L. Pyatigorskaya, Y.N. Venevtsev, Complete phase diagram of the $PbTiO_3$–$BiFeO_3$ system, Sov. Phys.-Solid State 6 (2) (1964) 375.
[2] R.T. Smith, G.D. Achenbach, R.W.J. James, Dielectric properties of solid solutions of $BiFeO_3$ with $Pb(Ti,Zr)O_3$ at high temperature and high frequency, J. Appl. Phys. 39 (1) (1968) 70.
[3] V.V.S.S.S. Sunder, A. Halliyal, A.M. Umarji, Investigation of tetragonal distortion in the $PbTiO_3$–$BiFeO_3$ system by high-temperature X-ray diffraction, J. Mater. Res. 10 (5) (1995) 1301.
[4] S.A. Fedulov, Y.N. Venevtsev, G.S. Zhdanov, E.G. Smazhevskaya, I.S. Rez, X-ray and electrical studies of the $PbTiO_3$–$BiFeO_3$ system, Sov. Phys.-Crystallogr. 7 (1) (1962) 62.
[5] R.J.D. Tilley, Principle and Applications of Chemical Defects, Stanley Thornes, Cheltenham, 1998.
[6] J.T.S. Irvine, D.C. Sinclair, A.R. West, Electroceramics: characterisation by impedance spectroscopy, Adv. Mater. 2 (3) (1990) 132.
[7] D.C. Sinclair, A.R. West, Impedance and modulus spectroscopy of semiconducting $BaTiO_3$ showing positive temperature coefficient of resistance, J. Appl. Phys. 66 (8) (1989) 3850.
[8] N.N. Krainik, N.P. Khuchua, V.V. Zhdanova, V.A. Evseev, Phase transitions in $BiFeO_3$, Sov. Phys.-Solid State 8 (3) (1966) 654.
[9] D.M. Smyth, Ionic transport in ferroelectrics, Ferroelectrics 151 (1994) 115.
[10] Y.H. Han, J.B. Appleby, D.M. Smyth, Calcium as an impurity in $BaTiO_3$, J. Am. Ceram. Soc. 70 (2) (1987) 96.
[11] A.R. West, Basic Solid State Chemistry, John Wiley and Sons, Chichester, 1999.
[12] M.V. Raymond, D.M. Smyth, Deffects and charge transport in perovskite ferroelectrics, J. Phys. Chem. Solids 57 (10) (1996) 1507.